

# The nature of the QCD plasma

Sourendu Gupta  
(TIFR, Mumbai)

LNF

7 March, 2006

The phase diagram, quasi-particles, constructing the effective theory.

Collaborators: Datta, Gavai, Lacaze, Mukherjee, Ray

# Plan

1. An introduction to the [phase diagram of QCD](#) and difficulties in computing it numerically.
2. Finding the [critical point of QCD](#): an outline of techniques, and the results.
3. Determining the [nature of excitations](#) in the plasma phase of QCD, i.e., the fields in terms of which a simple effective theory may be written.
4. Constraints on the [effective theory](#): crossover from chiral physics to a dimensionally reduced gauge-Higgs system.

# Global symmetries and order parameters

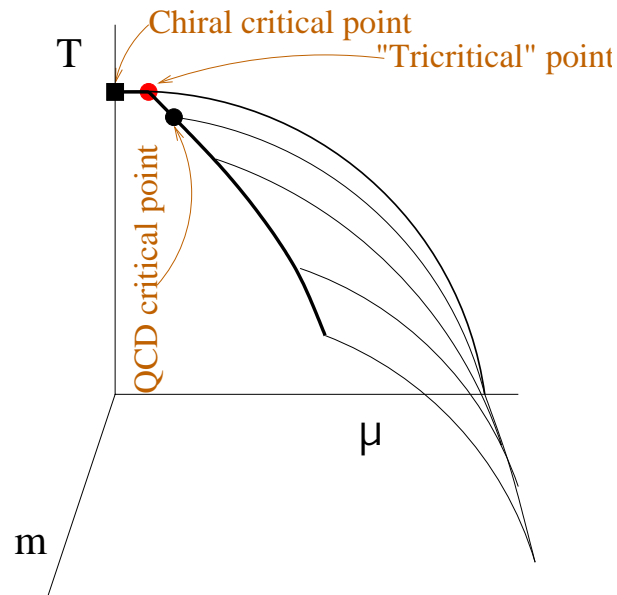
Two flavours of light quarks: approximate  $SU(2) \times SU(2)$  chiral symmetry, in the limit broken spontaneously to diagonal  $SU(2)$ , (pseudo) Goldstone bosons are the (light pseudo-scalar) pions.

Five tunable parameters:  $T$  (temperature),  $\mu_u$  and  $\mu_d$  (two chemical potentials),  $m_u$  and  $m_d$  (two masses). Gibbs phase rule allows large order multi-critical points.

Order parameter for chiral symmetry restoration:  $\langle \bar{\psi}\psi \rangle$ , tuned by changing  $T$  and  $\mu = (\mu_u + \mu_d)/2$ , excitations in this “radial” direction are heavy scalar mesons.

Order parameter for pion condensation:  $\langle \bar{\psi}\gamma_5\tau_2\psi \rangle$ , non-zero value may be induced by tuning isospin chemical potential  $\mu_3 = (\mu_u - \mu_d)/2$ , excitations in this direction give a massless charged pion.

# The phase structure



Berges and Rajagopal, Halasz, Jackson, Schrock, Stephanov and Verbaarschot: 1998

Section of the 5-d phase diagram along a surface of  $\mu_3 = 0$ : phases distinguished by  $\langle \bar{\psi}\psi \rangle$ . Other interestingly ordered phases at larger  $\mu$ .

Special symmetry for  $m_u = m_d$ — “tricritical” point is probably higher order. SG and Ray, in progress

# The sign problem

$$Z = e^{-F/T} = \int DU \, e^{-S} \prod_f \det M(U, m_f, \mu_f) = \int DU \, e^{-\mathcal{S}(T, \mu)}$$

where the Dirac operator is the staggered quark discretisation of  $M = m + \partial_\mu \gamma_\mu$ .

- If there is a  $Q$  such that  $M^\dagger = Q^\dagger M Q$ , then clearly  $\det M$  is real.
- $Q = \gamma_5$  for  $\mu = 0$ . Nothing for  $\mu \neq 0$ .
- Monte Carlo simulations of  $Z$  fail.
- Special cases:  $\mu$  pure imaginary,  $\mu_3$ ,  $N_c = 2$ .

## Avoiding the sign problem

- Reweighting: Simulate at some parameter set, reweight to another. Fodor and Katz (2001), Bielefeld-Swansea (2002)
- Imaginary chemical potential:  $\exp(i\mu)$  like a  $U(1)$  gauge field, no sign problem. d'Elia and Lombardo (2002), de Forcrand and Philipsen (2002), Azcoiti et al (2004)
- Taylor Expansion of free energy: Gavai and SG (2003), Bielefeld-Swansea (2003)

## The Taylor expansion for 2 flavours

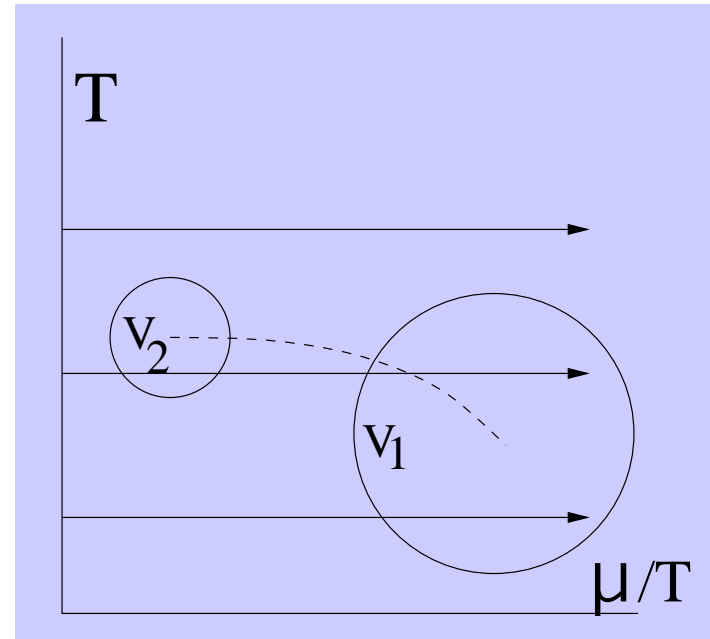
$$P(T, \mu_u, \mu_d) = \left( \frac{T}{V} \right) \log Z(T, \mu_u, \mu_d)$$

$$P(T, \mu_u, \mu_d) = P(T, 0, 0) + \sum_{n_u, n_d} \chi_{n_u, n_d} \frac{\mu_u^{n_u}}{n_u!} \frac{\mu_d^{n_d}}{n_d!}$$

$m_u = m_d$  implies that  $\chi_{n_u, n_d} = \chi_{n_d, n_u}$ ,  
for any  $\mu_u = \mu_d$ . One QNS is

$$\chi_B(T, \mu_B) = \left. \frac{\partial^2 P(T, \mu_u, \mu_d)}{\partial \mu_B^2} \right|_{\mu_u = \mu_d = \mu_B/3}$$

$\chi_B(T^E, \mu_B^E)$  diverges in the infinite  
volume limit: pseudo critical behaviour  
at finite volumes.



# Differential calculus by machine: 1

There are mechanical and (**almost**) fully programmable methods to take the derivatives involved in a high-order Taylor series expansion of the partition function with fermions and finding the most efficient way of programming the Taylor coefficients.

## Step 1

Relate the derivatives of  $\log Z$  to the derivatives of  $Z$ . Trivially accomplished by, e.g., the simple Mathematica program

$$\text{chi}[n\_ , m\_ ] := D[ \text{Log}[Z[u, d]], \{u, n\}, \{d, m\}],$$

or its generalization to a larger number of flavours. Notation used is

$$\chi_{nm} = \chi_{\underbrace{uu\dots}_{n \text{ times}} \underbrace{dd\dots}_{m \text{ times}}}$$



## Differential calculus by machine: 2

### Step 2

Relate the derivatives of  $Z$  to fermion traces. As long as we work with equal mass flavours, the fermion traces are flavour independent. Introduce the notation

$$Z_{10} = Z \langle \mathcal{O}_1 \rangle, \quad \mathcal{O}'_n = \mathcal{O}_{n+1}.$$

Use the rule  $[\det M]' = [\exp \text{Tr} \log M]' = \text{Tr} M' M^{-1} \det M$ , to write

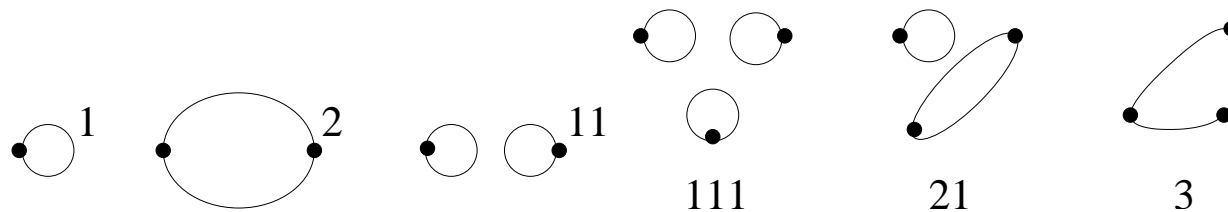
$$Z_{10} = Z_{01} = \frac{\partial Z}{\partial \mu_f} = \int DU e^{-S} \text{Tr } M_f^{-1} M'_f.$$

Note:  $M' = \gamma_0$  and  $M^{-1} = \psi \bar{\psi}$ , so  $\text{Tr } M^{-1} M' = \psi^\dagger \psi$ . S. Gottlieb *et al.*, *Phys. Rev. Lett.*, 59 (1987) 2247

# Differential calculus by machine: 3

## Step 3

Use the chain rule to write down higher order derivatives in terms of the  $\mathcal{O}_n$  and their products. A diagrammatic representation of these quantities is possible, and can be used to check the results. [SG, Zakopane lectures, 2002](#)



Example:  $Z_{60}$  contains  $\mathcal{O}_{1122}$  with coefficient equal to the number of ways of partitioning 6 objects into groups of 2 ones and 2 twos, i.e.,

$$\left\{ \frac{1}{2} \binom{6}{1} \binom{5}{1} \right\} \times \left\{ \frac{1}{2} \binom{4}{2} \right\} = 45.$$

## Differential calculus by machine: 4

### Step 4

The diagrams still have to be related to fermion traces. In the continuum this is trivial because only  $M' = \gamma_0 \neq 0$ . On the lattice there are several more steps, since arbitrary derivatives,  $M^{(p)}$ , exist. Introduce further notation

$$[n_1 \cdot p_1 \oplus n_2 \cdot p_2 \oplus \dots] = \text{Tr} \left[ \left( M^{-1} M^{(p_1)} \right)^{n_1} \left( M^{-1} M^{(p_2)} \right)^{n_2} \dots \right].$$

Then derivatives are given by the rule—

$$[n \cdot p]' = -n[1 \oplus n \cdot p] + n[(n-1) \cdot p \oplus (p+1)].$$

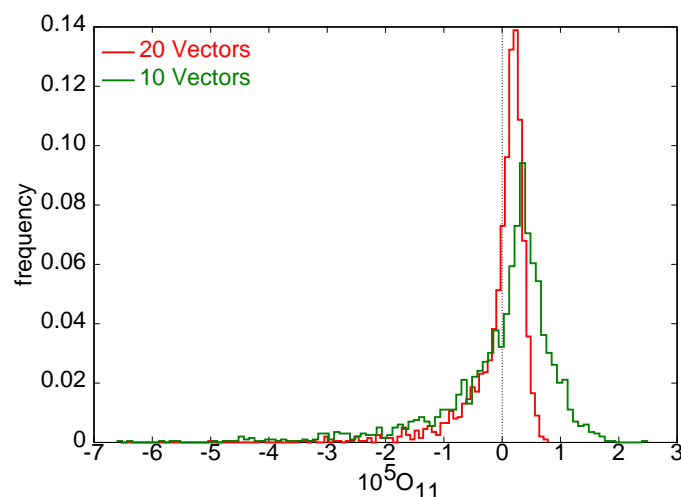
The chain rule is equivalent to making the derivative linear over  $\oplus$ .

Example:  $[1] = \text{Tr} M^{-1} M'$ , and  $[1]' = -[2 \cdot 1] + [2]$ .

# Differential calculus by machine: 5

## Step 5

Numerical estimates of traces are made by the usual noisy method, which involves the identity  $I = \overline{|r\rangle} \langle r|$ , where  $r$  is a vector of complex Gaussian random numbers. We need upto 500 vectors in the averaging.

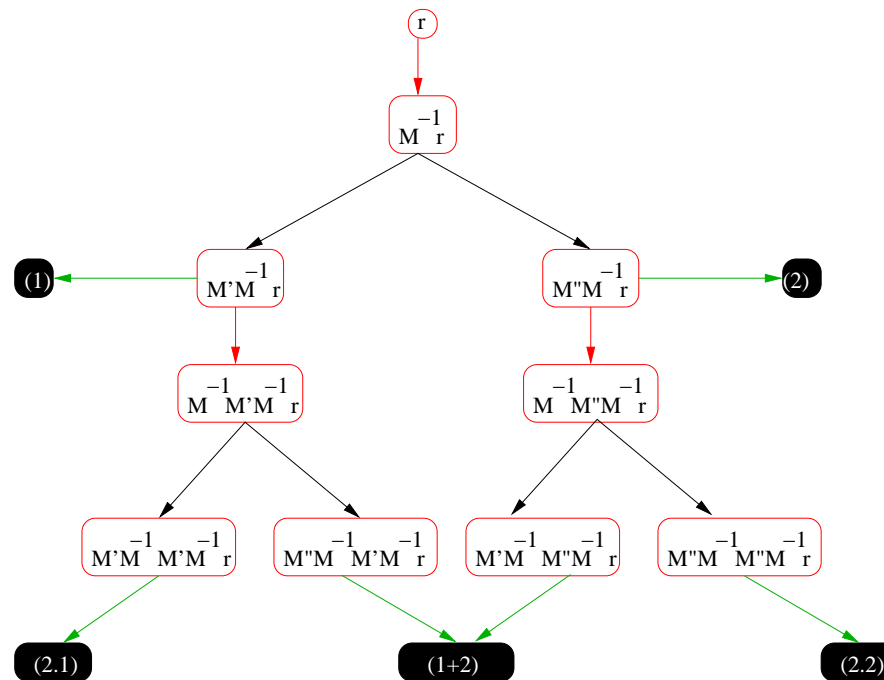


The histogram of  $O_{11}$  where  $\chi_{ud} = \langle O_{11} \rangle$ . In the limit of infinite number of vectors the histogram should be skew, a tail to the left and vanishing abruptly at zero.

# Differential calculus by machine: 6

## Step 6

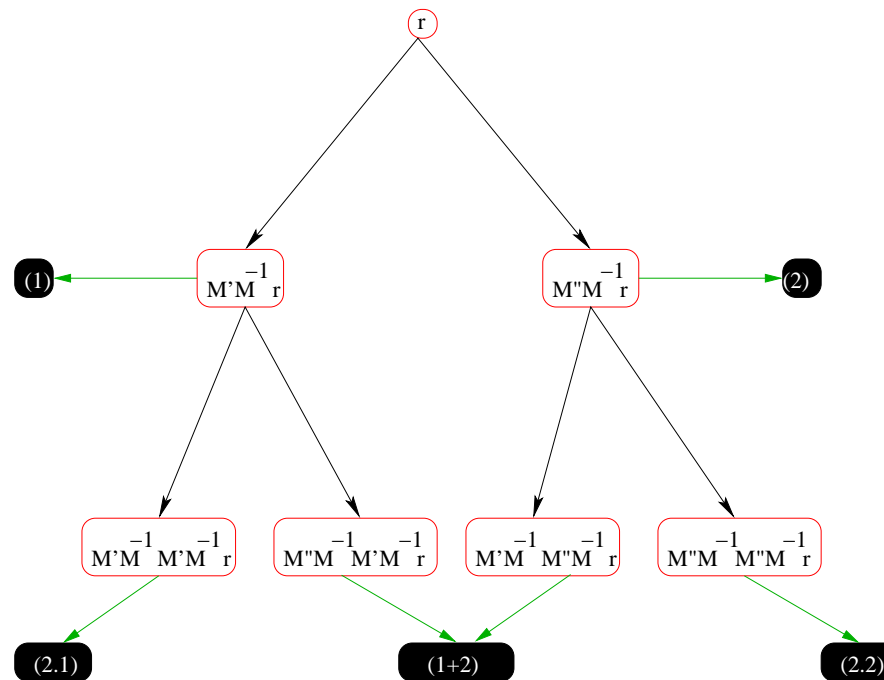
Optimisation of the computation of multiple traces reduces to an NP-complete problem in computer science called the **Steiner problem**. Need 20 matrix inversions to perform a single measurement of upto 8th order susceptibilities.



# Differential calculus by machine: 6

## Step 6

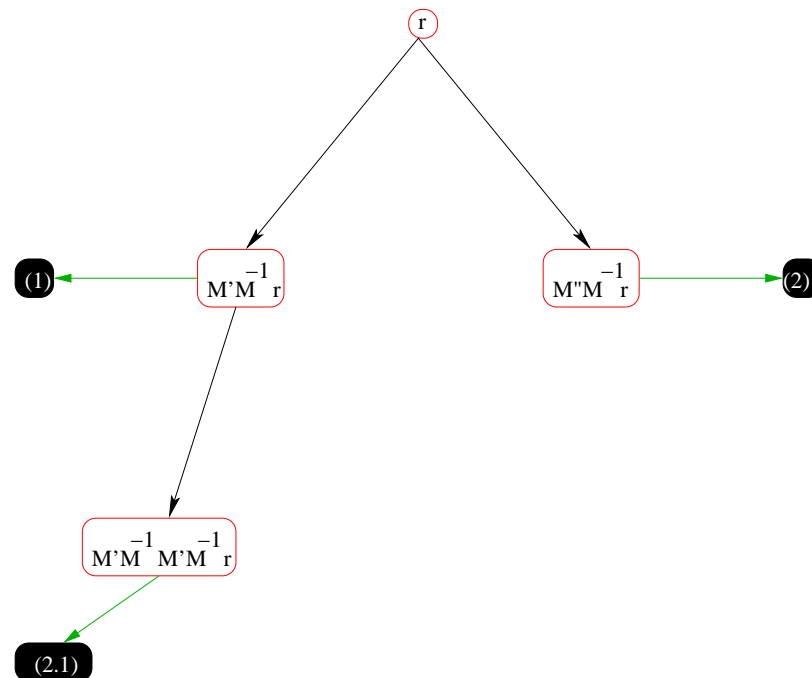
Optimisation of the computation of multiple traces reduces to an NP-complete problem in computer science called the **Steiner problem**. Need 20 matrix inversions to perform a single measurement of upto 8th order susceptibilities.



# Differential calculus by machine: 6

## Step 6

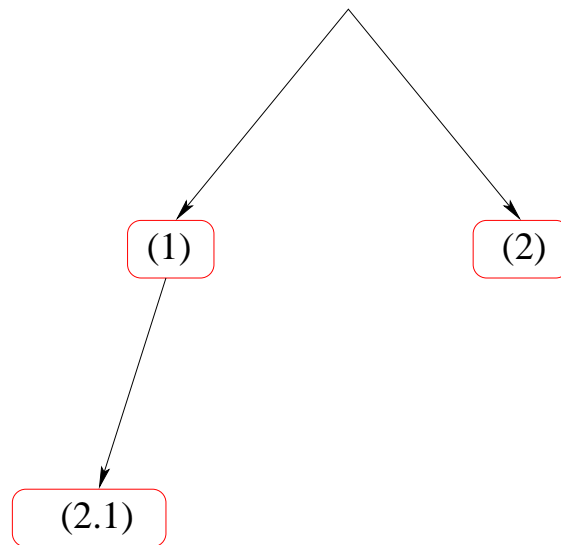
Optimisation of the computation of multiple traces reduces to an NP-complete problem in computer science called the **Steiner problem**. Need 20 matrix inversions to perform a single measurement of upto 8th order susceptibilities.



# Differential calculus by machine: 6

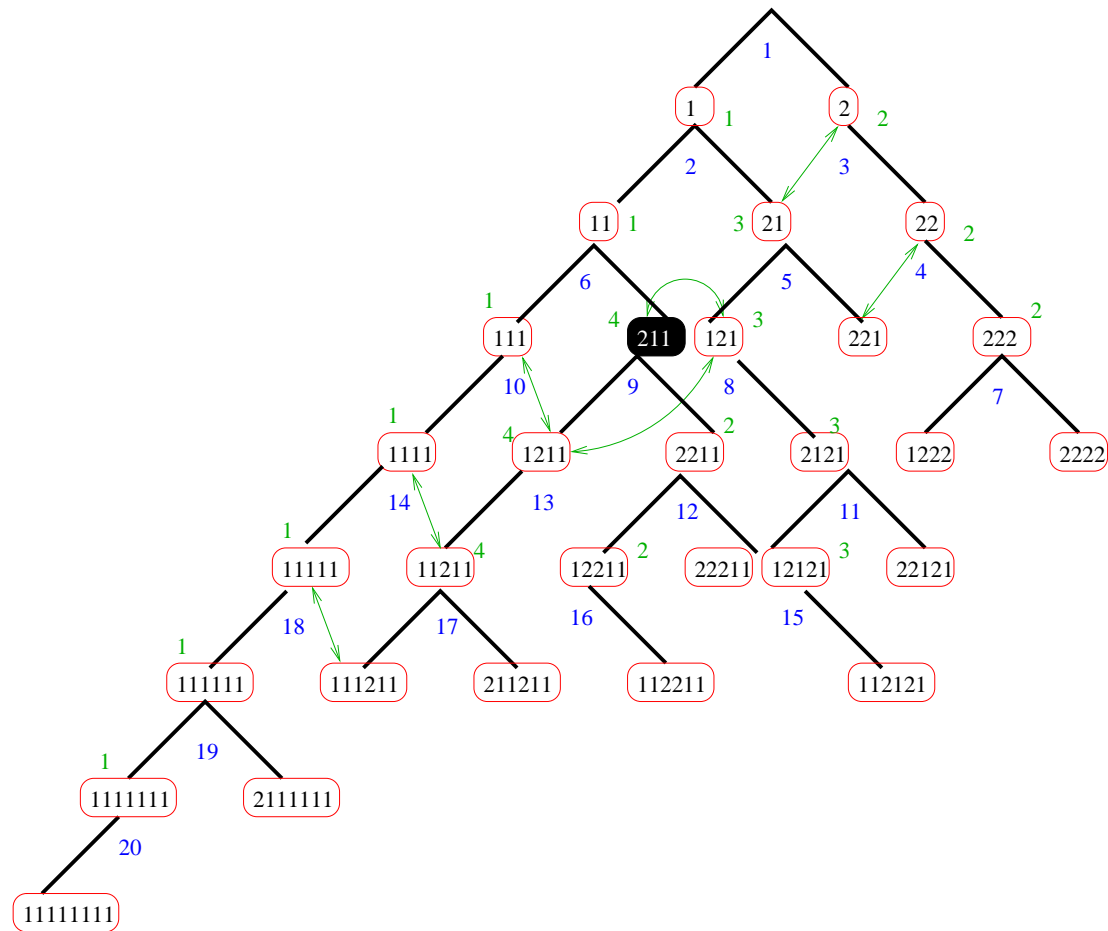
## Step 6

Optimisation of the computation of multiple traces reduces to an NP-complete problem in computer science called the **Steiner problem**. Need 20 matrix inversions to perform a single measurement of upto 8th order susceptibilities.



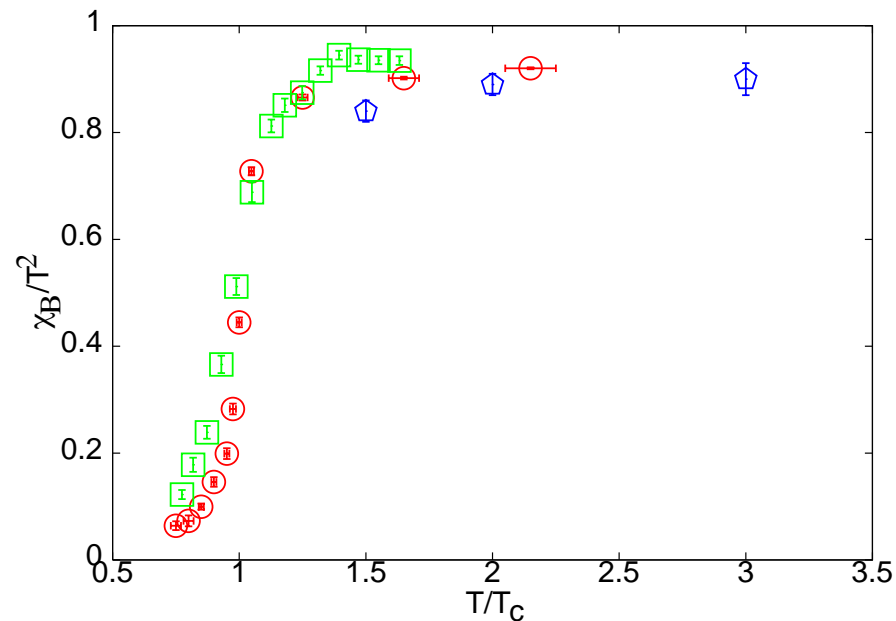


# The actual evaluation tree



Note the accuracy checks built into the optimal computation.

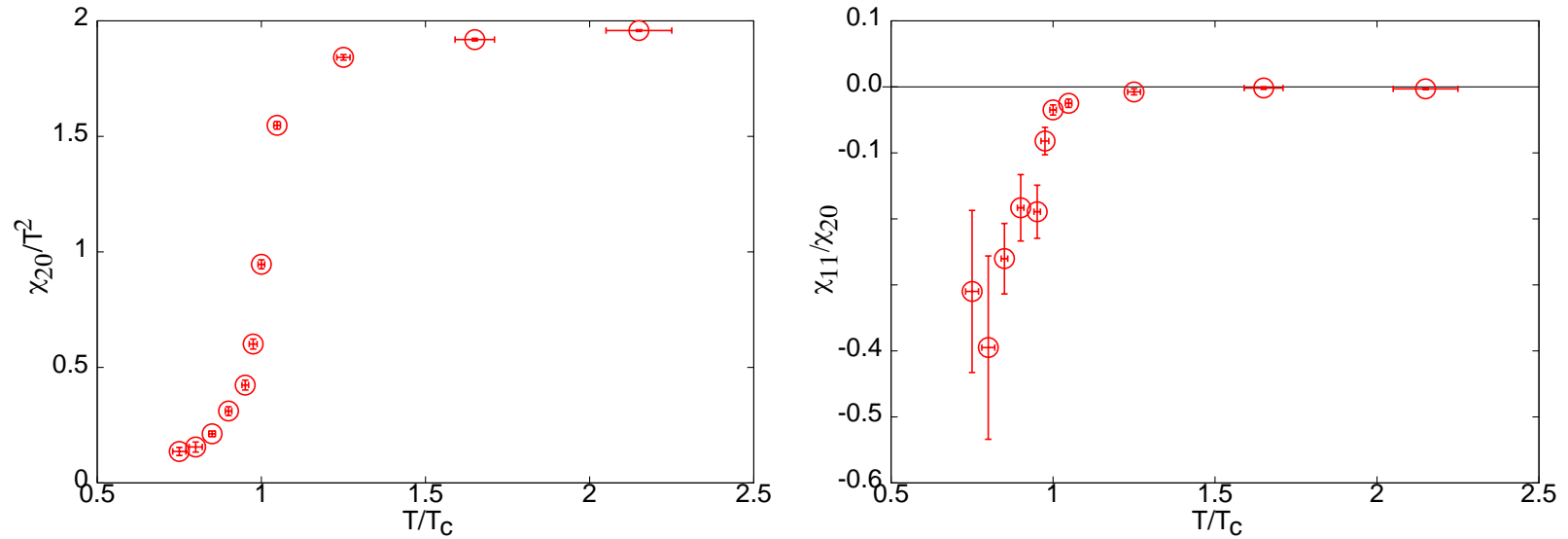
# Fluctuations



Quenched continuum (Mumbai), MILC  $a = 1/8T$ ,  $N_f = 2$ , Mumbai  $N_f = 2$   
continuum extrapolation through quenched

Weak coupling expansion: Blaizot, Iancu and Rebhan, Vuorinen

## The susceptibilities: sign fluctuations



$\chi_{20}$  measures the spread of quark numbers in the real direction, and  $\chi_{11}$  its spread in the imaginary direction. Increasing ratio  $|\chi_{11}|/\chi_{20}$  shows increasing severity of the sign problem.

## Non-linear susceptibilities

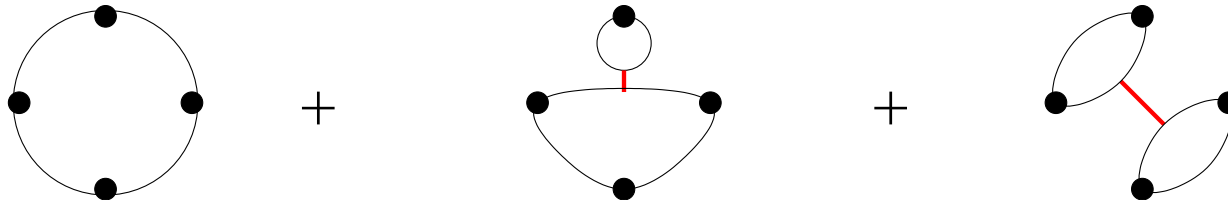
A non-linear quark number susceptibility of order  $n$  is the derivative

$$\chi_B^{(n)} = \frac{\partial^n P}{\partial \mu_B^n} \quad \text{and} \quad \chi_{n_u, n_d} = \frac{\partial^{n_u + n_d} P}{\partial \mu_u^{n_u} \partial \mu_d^{n_d}}$$

Now,

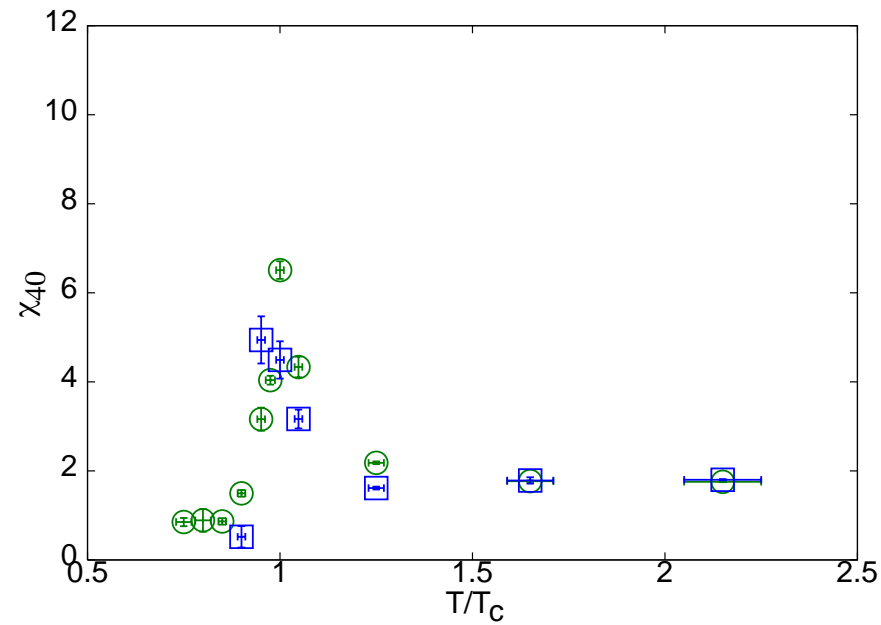
$$\chi_B^{(4)} = \frac{1}{2} [\chi_{40} + 2\chi_{31} + \chi_{22}]$$

In terms of quarks, we have:



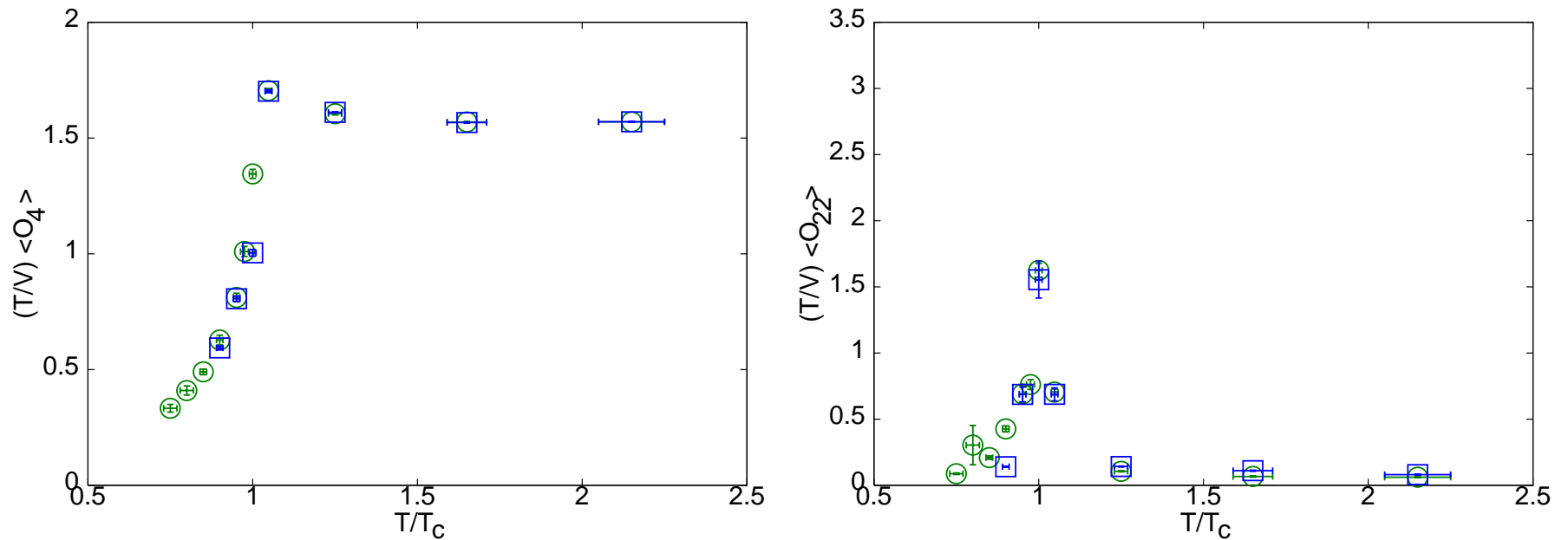
Flavour disconnected pieces are absent for free quarks, i.e., vanish when  $g \rightarrow 0$ . In a resonance gas one has vertices such as  $\pi^+ + \pi^- \rightarrow \pi^0 + \pi^0$  which allow the flavour disconnected pieces to add up.

## Peaking at $T_c$



Peak in  $\chi_B^{(4)}$  implies decrease in radius of convergence  $r_{2/4} = \sqrt{\chi_B^{(2)}/\chi_B^{(4)}}$ .

## Resolving the peak

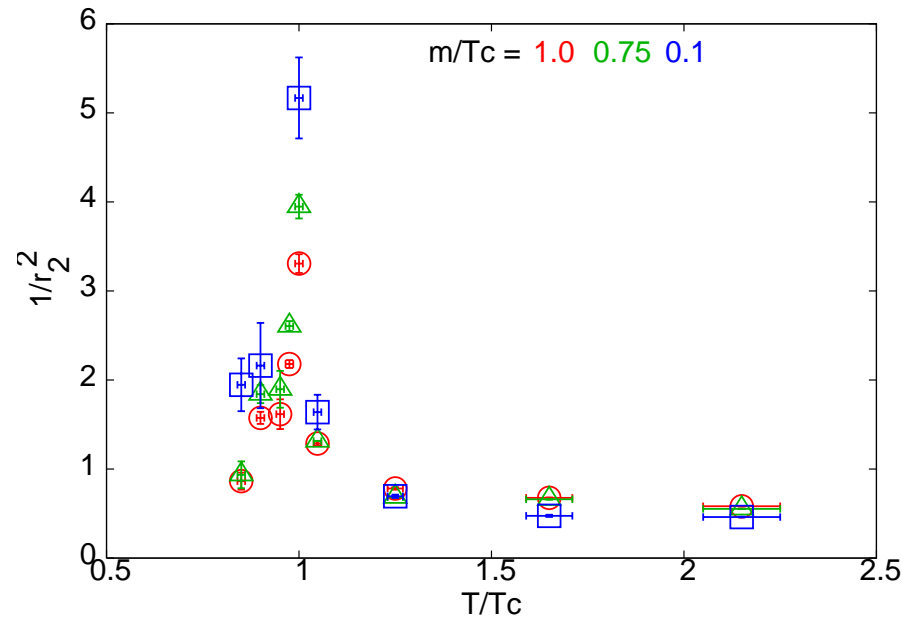


Peaks in other susceptibilities also found very close to  $T_c$ . Always in  $O_{22}$ ,  $O_{222}$ ,  $O_{2222}$ — i.e., quark line disconnected operators  $(\text{Tr } \gamma_0 D \gamma_0 D)^n$ .

R. V. Gavai and SG, PRD 72 (2005) 054007

## Quark mass dependence

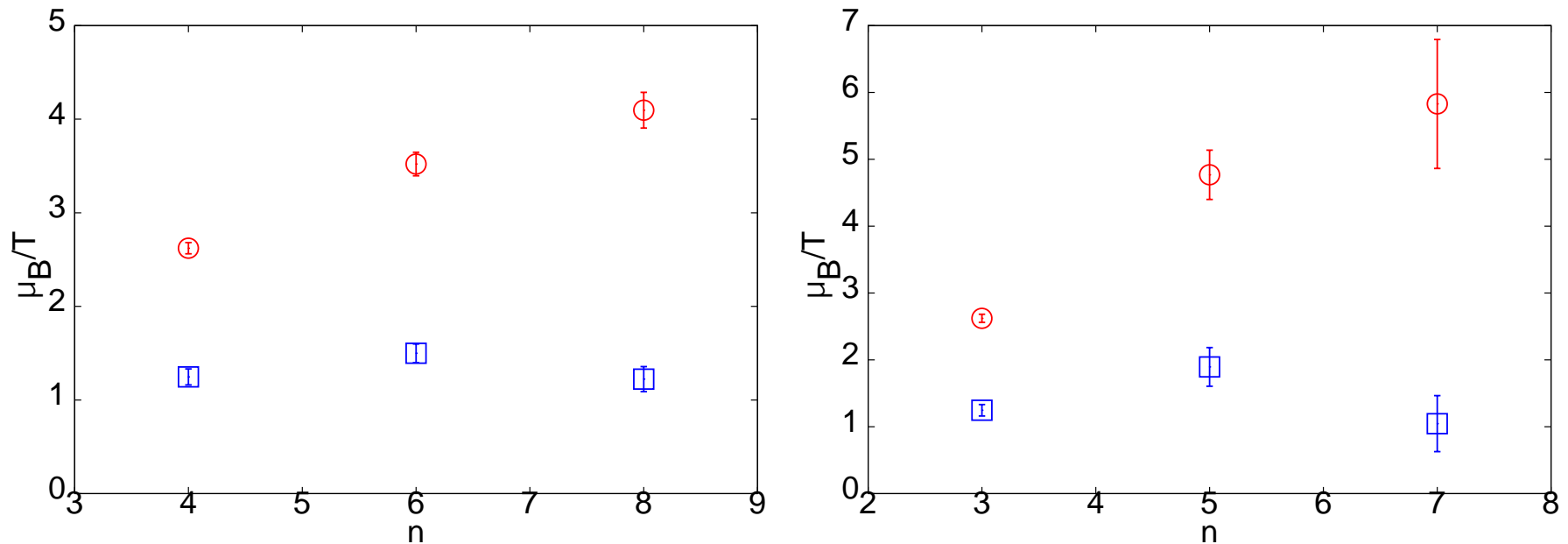
Peak in  $\chi_{40}$  etc., implies decreasing radius of convergence. The radius of convergence seems to be very sensitive to quark mass in some region of  $T$ .



With increasing order larger there is a slower approach to the infinite volume limit, and a threshold  $Lm_\pi \approx 5$  is needed to study the thermodynamic limit.

# Radius of convergence

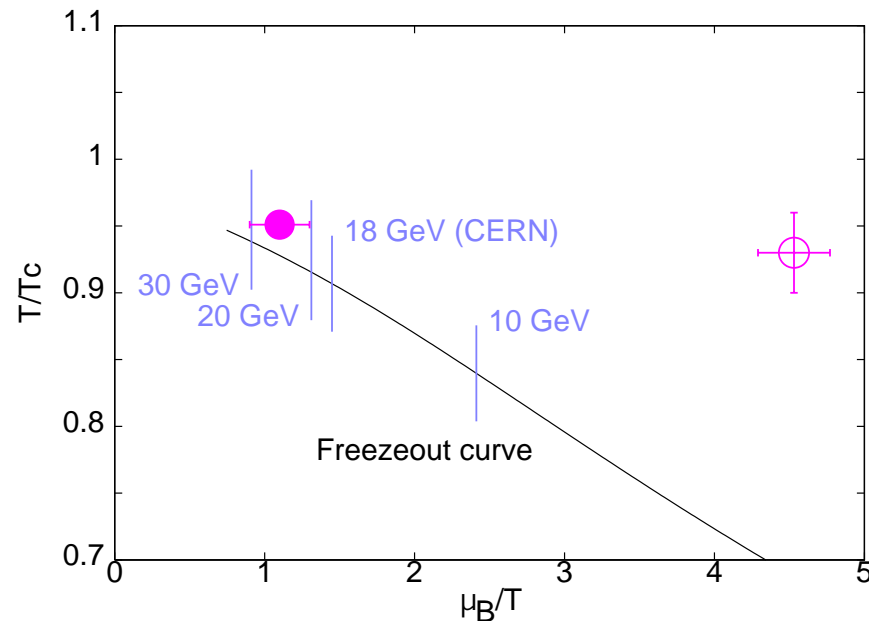
Notation: If  $f(x) = \sum_n f_{2n} x^{2n}$  then  $\rho_{2n} = \left| \frac{f_0}{f_{2n}} \right|^{1/2n}$  and  $r_{2n+1} = \sqrt{\left| \frac{f_{2n}}{f_{2n+2}} \right|}$



Old Budapest results roughly consistent with our small volume analysis.



# The QCD critical end point



R. V. Gavai and SG, PRD 71 (2005) 114014

Strong finite volume effect; strong quark mass effect. When  $Lm_\pi \rightarrow \infty$ ,  $a = 1/4T$  and  $m_\pi/m_\rho = 0.3$  then  $T^E/m_\rho \approx 0.17$  and  $\mu^E/m_\rho \approx 0.20$ .

## Summary of phase diagram

1. Sign problem under reasonable control in QCD for  $T/m_\rho > 0.13$ .
2. Taylor expansion can be used to explore the phase diagram upto the nearest singularity to the  $\mu = 0$  starting point.
3. Extrapolation to infinite volume has pitfalls: careful.
4. With  $a = 1/4T$  and  $m_\pi/m_\rho = 0.3$  one finds  $T^E/m_\rho \approx 0.17$  and  $\mu^E/m_\rho \approx 0.20$ .
5. Strong dependence on quark mass, i.e.,  $m_\pi/m_\rho$ .

## Quasiparticles: linkage of quantum numbers

Since there are many conserved quantum numbers the problem becomes simpler. Look at two quantum numbers simultaneously— say  $U$  and  $D$ .

$T < T_c$ : whenever  $U = 1$  is excited  $D = -1$  is excited along with it.

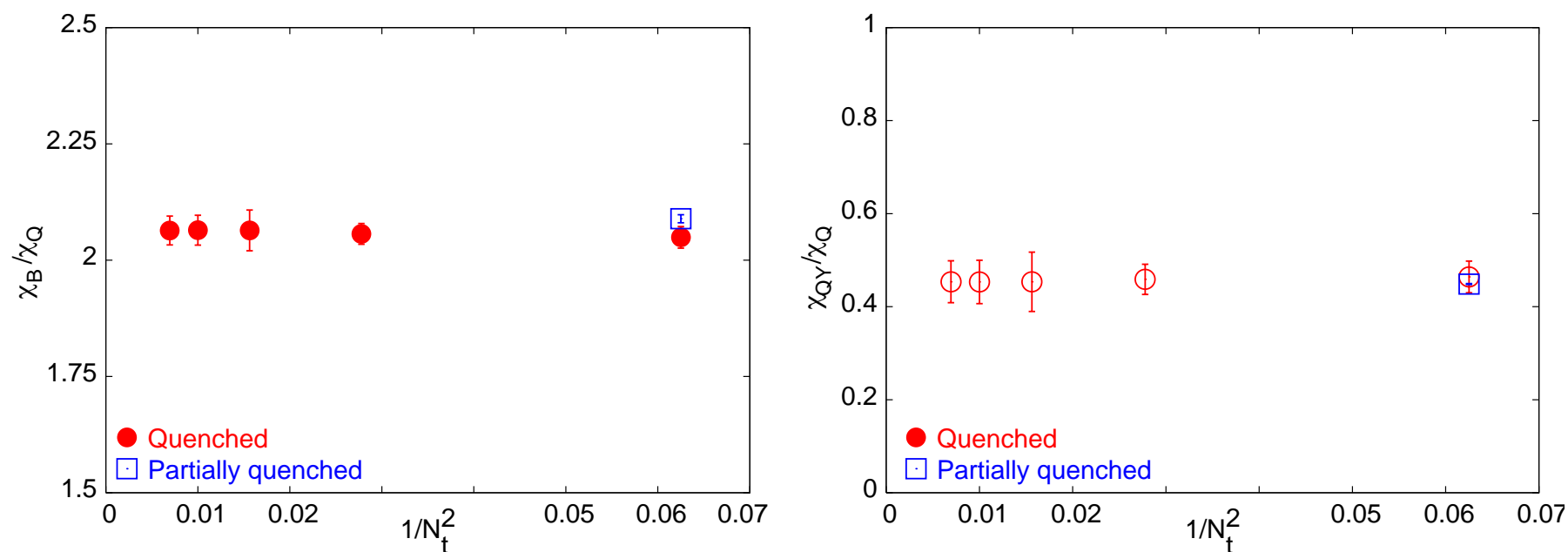
$T > T_c$ : when  $U = 1$  is excited  $D = \pm 1$  should be excited along with it if the medium contains quarks. Otherwise, by observing what value of  $D$  is preferentially excited, you find something about the quantum numbers of the excitations.

Similarly one could study the **linkages**  $U|B$  or  $U|Q$ , or  $D|B$  etc.

$$C_{(XY)/Y} \equiv \frac{\langle XY \rangle - \langle X \rangle \langle Y \rangle}{\langle Y^2 \rangle - \langle Y \rangle^2} = \frac{\chi_{XY}}{\chi_Y}$$

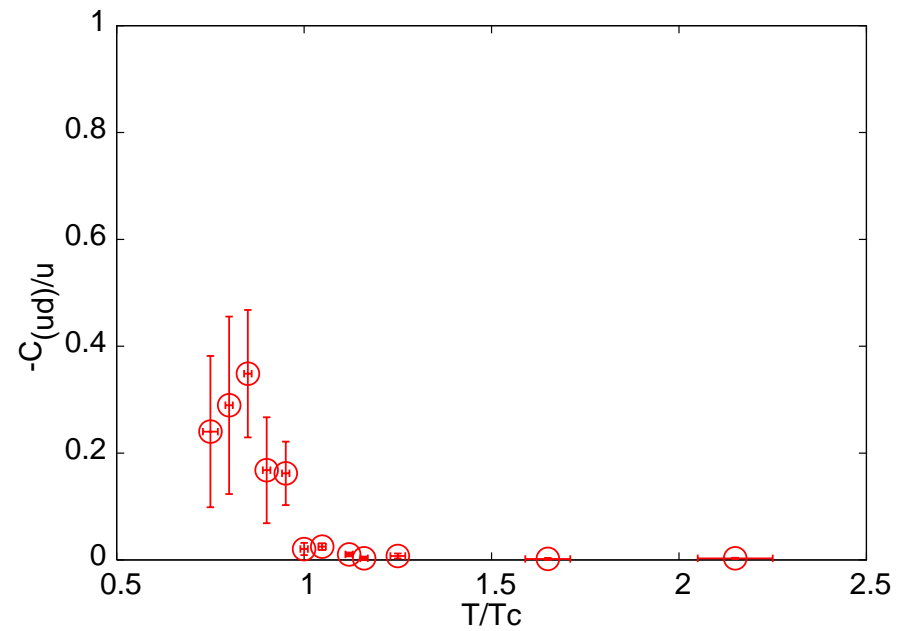
Gavai and SG, PRD 73 (2006) 014004

## Linkage is robust



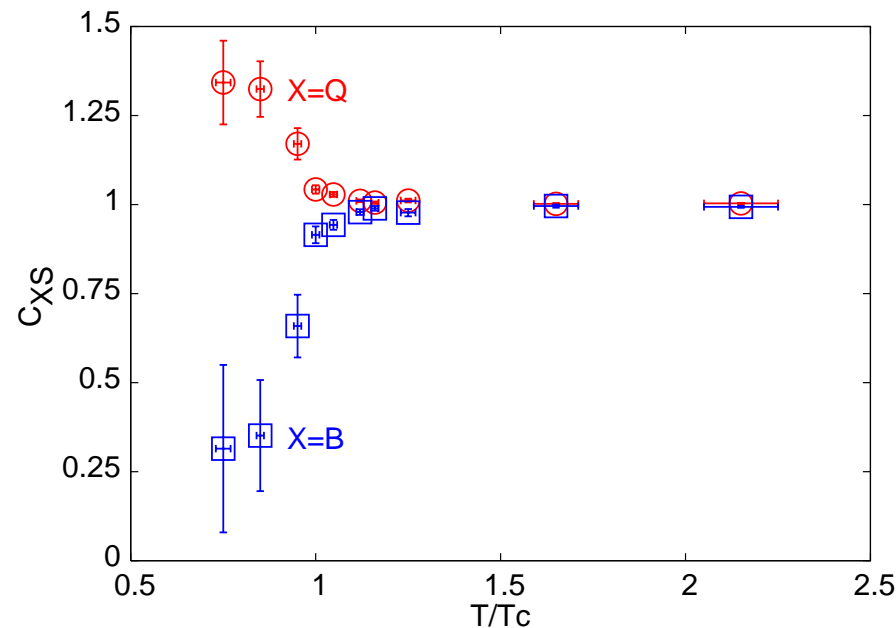
Above  $T_c$  ratios of QNS are almost independent of lattice spacing, and insensitive to quark masses (as long as  $m < T$ ). Therefore linkage is a robust quantity above  $T_c$ .

## U and D are not linked



$u$  and  $\bar{d}$  can be carried by the same particle below  $T_c$  but not above  $T_c$ .

## Strangeness is carried by quarks

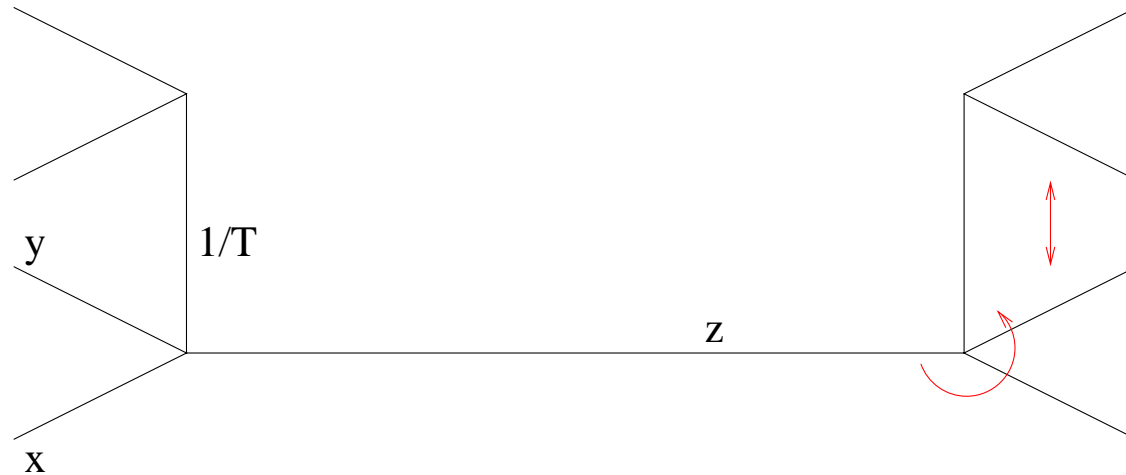


$C_{BS} = -3C_{(BS)|S}$  and  $C_{QS} = 3C_{(QS)|S}$ . Below  $T_c$  strange baryons are relatively heavy and therefore sparse in the plasma, but kaons are not so heavy. Above  $T_c$ : strange quarks.

Gavai and SG, Koch, Majumder, Randrup, PRL 95 (2005) 182301

## Glue sector: screening masses

Since gluons do not carry any global quantum numbers, one cannot apply the same methods to examine gluon-sector quasi particles. Instead it is investigated through screening masses of colour singlets: sometimes called “glueball” correlations.

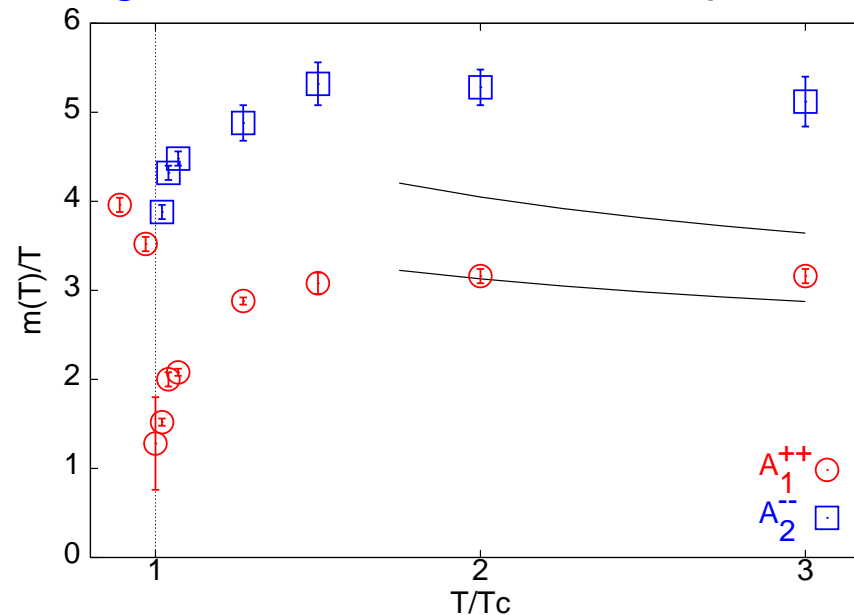


$J^{PC}$  breaks down to  $\mathcal{M}^{Tc}$ . Measure—

$$C_{\mathcal{M}^{Tc}}(z) \propto \exp[-zm(\mathcal{M}^{Tc})].$$

# Gluon sector screening masses (I)

Electric gluons at finite temperature have lattice quantum number  $1^{--}$  and colour quantum numbers. Colour singlet **two gluon** states have lattice quantum number  $0^{++}$ . Colour singlet **three gluon** states have lattice quantum number  $1^{--}$ .

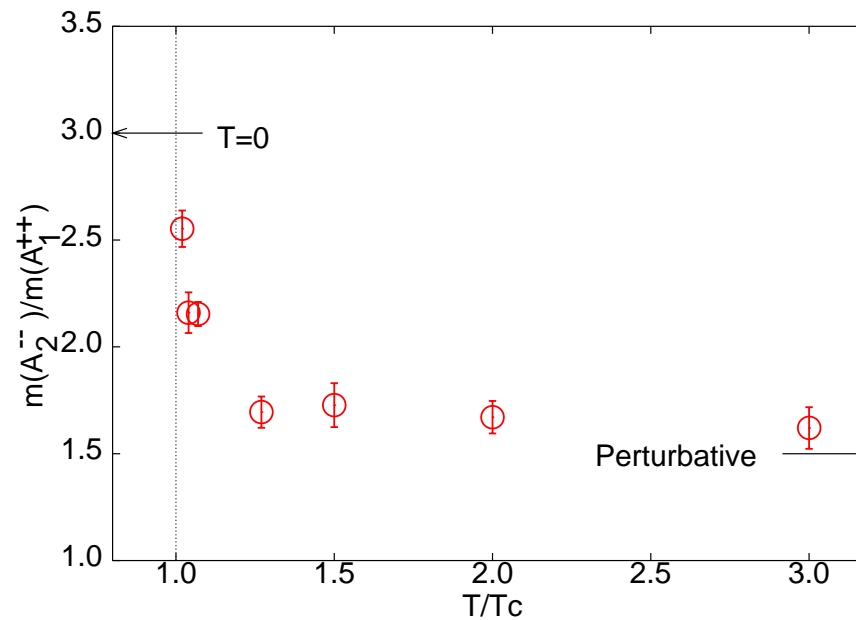


Comparison with weak-coupling prediction ( $m/T \propto g + \dots$ ) spoiled by scale uncertainty. **Datta and SG, Phys.Rev.D67 (2003) 054503**



## Gluon sector (II)

Ratio of the two masses provides a test of whether weakly coupled gluons is a valid picture. Less affected by scale uncertainties if  $g$  is small enough, since  $m/m' \propto 3/2 + \dots$ .



Works (qualitatively) at  $T/T_c \geq 1.25$ . Fails below that.

## Summary of 2nd part

1. Immediately above the crossover, **quark quasi-particles** can be observed in the QCD plasma. Linkage is usually visible in experiments— called particle id, when single particles can be tagged in detector. In plasma need to use linkage as defined.
2. Above  $1.25T_c$  **gluon quasi-particles** visible in plasma. Since they carry no conserved global (internal) quantum numbers, they are difficult to identify near  $T_c$ .
3. There is emerging evidence of interesting structure in the gauge fields which strongly influence the spectrum of the Dirac operator through the creation of localized eigenstates of quarks.